



Molecular Crystals and Liquid Crystals Science and Technology. Section A. Molecular Crystals and Liquid Crystals

Publication details, including instructions for authors and
subscription information:

<http://www.tandfonline.com/loi/gmcl19>

Splayed TN Configuration Stability in Domain-Divided TN Mode

Ken-Ichi Takatori^a & Ken Sumiyoshi^a

^a Functional Devices Research Laboratories, NEC Corporation, 4-1-1,
Miyazaki, Miyamae-ku, Kawasaki, Kanagawa, 216, Japan
Version of record first published: 23 Sep 2006.

To cite this article: Ken-Ichi Takatori & Ken Sumiyoshi (1995): Splayed TN Configuration Stability in Domain-Divided TN Mode, Molecular Crystals and Liquid Crystals Science and Technology. Section A. Molecular Crystals and Liquid Crystals, 263:1, 445-458

To link to this article: <http://dx.doi.org/10.1080/10587259508033604>

PLEASE SCROLL DOWN FOR ARTICLE

Full terms and conditions of use: <http://www.tandfonline.com/page/terms-and-conditions>

This article may be used for research, teaching, and private study purposes. Any substantial or systematic reproduction, redistribution, reselling, loan, sub-licensing, systematic supply, or distribution in any form to anyone is expressly forbidden.

The publisher does not give any warranty express or implied or make any representation that the contents will be complete or accurate or up to date. The accuracy of any instructions, formulae, and drug doses should be independently verified with primary sources. The publisher shall not be liable for any loss, actions, claims, proceedings, demand, or costs or damages whatsoever or howsoever caused arising directly or indirectly in connection with or arising out of the use of this material.

SPLAYED TN CONFIGURATION STABILITY IN DOMAIN-DIVIDED TN MODE

KEN-ICHI TAKATORI, KEN SUMIYOSHI
Functional Devices Research Laboratories,
NEC Corporation, 4-1-1, Miyazaki, Miyamae-ku, Kawasaki,
Kanagawa, 216, Japan

Abstract

In the domain-divided TN mode for a wide-viewing-angle LCD, the LC directors are arranged in the splayed TN configuration by mismatching the pretilt directions on both substrates. For this mismatched pretilt alignment, the splayed TN configuration and the reversely-twisted TN configuration are possible. It is shown that the reversely-twisted TN is more stable than the splayed TN in the high voltage range. The splayed TN stability proved to be evaluated by the balanced voltage, defined as voltage at which LC bulk energy becomes equal for two configurations in a simulation or voltage at which the boundary between two configurations is fixed in an experiment. Narrow twist angle, short chiral pitch and low pretilt angles raise the balanced voltage, i.e., stabilize the splayed TN configuration.

INTRODUCTION

The domain-divided Twisted Nematic Liquid Crystal Displays, the domain-divided TN LCDs^{1,2} (to avoid misunderstanding, the word "multi-domain TN" is used instead of "domain-divided TN" in this manuscript), are now attractive devices for improving a contrast angular dependence for conventional TN LCDs. In this multi-domain TN, each pixel has two or more director configuration domains, where individual pretilt directions differ. Such a configuration averages the conventional TN transmittances in various directions and therefore shows a good opto-electric characteristic in a wide viewing angle range. Nevertheless, this multi-domain TN LCD adds the fabrication process.

Some new structures^{3,4,5} having a splayed TN configuration have been proposed to reduce the number of additional process. In these structures, the pretilt directions on both substrates are mismatched. Moreover, a pretilt angle on the top substrate is not generally equal to that on the bottom one. While a matched pretilt alignment causes only conventional TN configuration, shown in Figure 1 (a), this mismatched pretilt alignment causes two possible configurations: one is the splayed TN configuration and the other is a reversely-twisted TN configuration. In the splayed TN, shown in Figure 1 (b), LC directors twist towards a chiral dopant sense, but the pretilt directions on both substrates don't agree with each other. On the contrary, in this configuration, shown in Figure 1 (c), the directors twist against the chiral dopant sense, but the pretilt directions on both substrates agree with each other. The splayed TN configuration in the multi-domain TN is observed to be easily deformed into the reversely-twisted TN configuration.

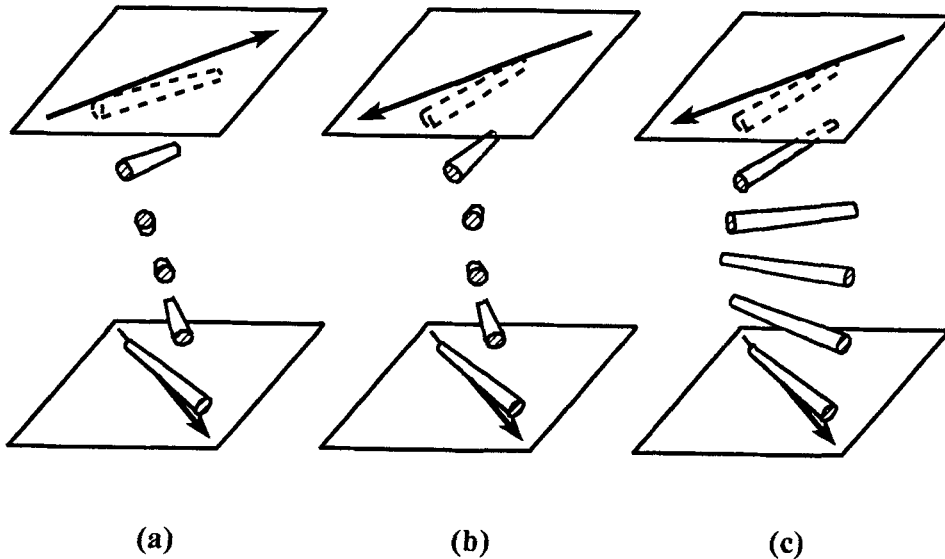


FIGURE 1 LC director configurations for (a) TN, (b) splayed TN and (c) reversely-twisted TN. The arrows represent the rubbing directions.

In the present work, the stability of the splayed TN configuration was studied with simulations and experiments.

DOMAIN STABILITY SIMULATION IN SPLAYED TN

First, the splayed TN cell was examined by simulations as a simple model to use in investigating the domain stability.

Simulation method

The Frank free energies on the one-dimensional electrical field system⁶ were calculated for the two configurations, the splayed TN (Figure 1 (b)) and the reversely-twisted TN (Figure 1 (c)). From the calculation results, the LC bulk elastic energies for two types are compared.

Figure 2 shows an example of the calculated energies for the splayed TN pretilted asymmetrically on the top and bottom substrates: chiral pitch(p_0)=50 μm , twist

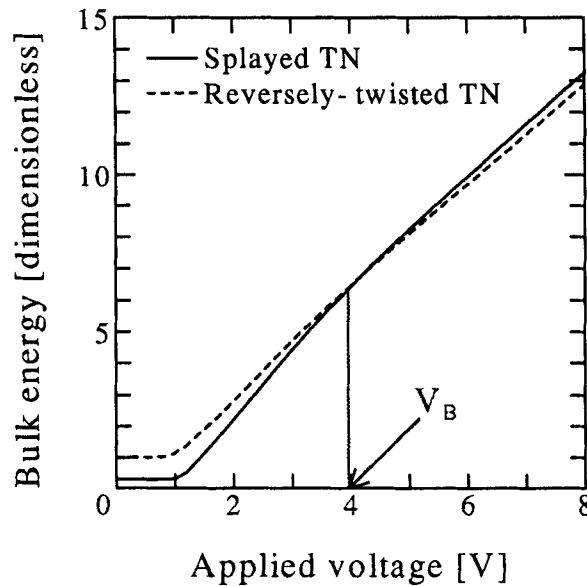


FIGURE 2 An example of calculated LC bulk energies for two configurations as a function of applied voltage. In the calculation, values were set at $p_0=50\mu\text{m}$, $\Phi=100^\circ$, $\theta_T=1.5^\circ$ and $\theta_B=3.0^\circ$.

angle(Φ)=100°, top pretilt angle(θ_t)=1.5° and bottom pretilt angle(θ_b)=3.0° were set. Those energies are normalized by the d/K_{11} and dimensionless, where d [μm] is the cell gap and K_{11} [N] is the Frank splay elastic constant. When the voltage is low, the splayed TN, represented by the solid line has lower energy than the reversely-twisted TN, represented by the dashed line. However, two bulk energies cross at about 4V: the energy inversion occurs at that voltage, which the authors call balanced voltage V_B .

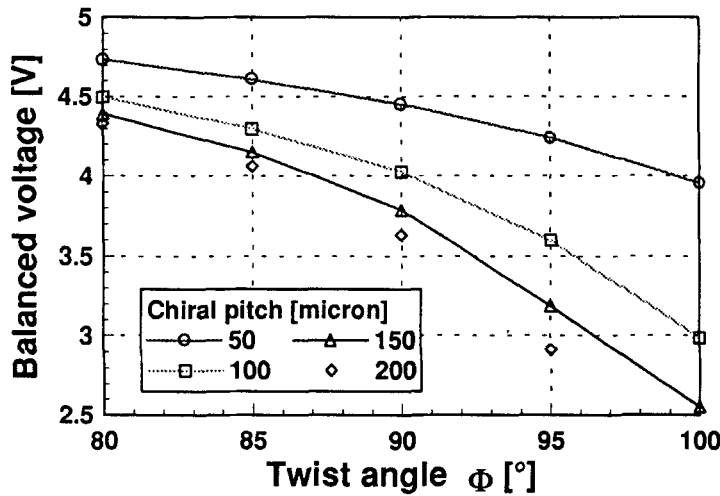


Figure 3 The balanced voltage in the simulation as a function of twist angle and chiral pitch with $\theta_t=1.5^\circ$ and $\theta_b=3.0^\circ$.

Effective parameters in energy inversion

The following parameters were examined in the simulation: the cell gap(d), the twist angle(Φ), the chiral pitch(p_0) and the pretilt angles(θ_t and θ_b). Based on the calculation results, it has been clarified that the cell gap doesn't affect the energy inversion. In contrast to this, other parameters do affect it.

Figure 3 shows the balanced voltages obtained by the simulation as a function of twist angle and chiral pitch for the splayed TN pretilted asymmetrically with $\theta_t=1.5^\circ$

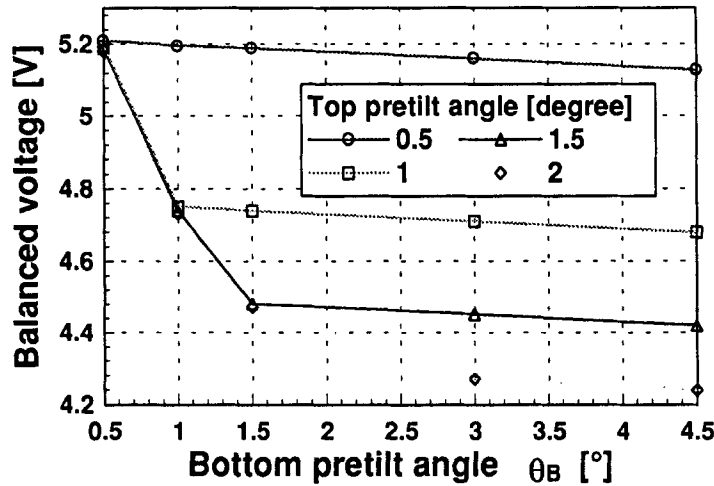


Figure 4 The balanced voltage in the simulation as a function of top and bottom pretilt angles with $p_0=50\mu\text{m}$, $\Phi=90^\circ$.

and $\theta_B=3.0^\circ$. When $\Phi=100^\circ$ and $p_0=200\mu\text{m}$, the splayed TN has lower energy than the reversely-twisted TN from 1.4V to 2.3V. As Figure 3 indicates, the shorter chiral pitch and the narrower twist angle stabilize the splayed TN configuration.

Figure 4 shows the balanced voltages on the simulation as a function of pretilt angles (θ_T and θ_B) with $\Phi=90^\circ$ and $p_0=50\mu\text{m}$. Figure 4 indicates that lower pretilt angle on either substrate stabilizes the splayed TN configuration.

DOMAIN-DIVIDED TN STABILITY EVALUATION FROM EXPERIMENTS

In this section, first we describe the domain stability measurement method.

Transition observation & LC configuration identification

The instruments, shown in Figure 5, were used to observe the domain transition. The polarizing microscope (1) is used for the conventional crossed-Nicols or parallel-Nicols observation and for getting conoscopic figures.

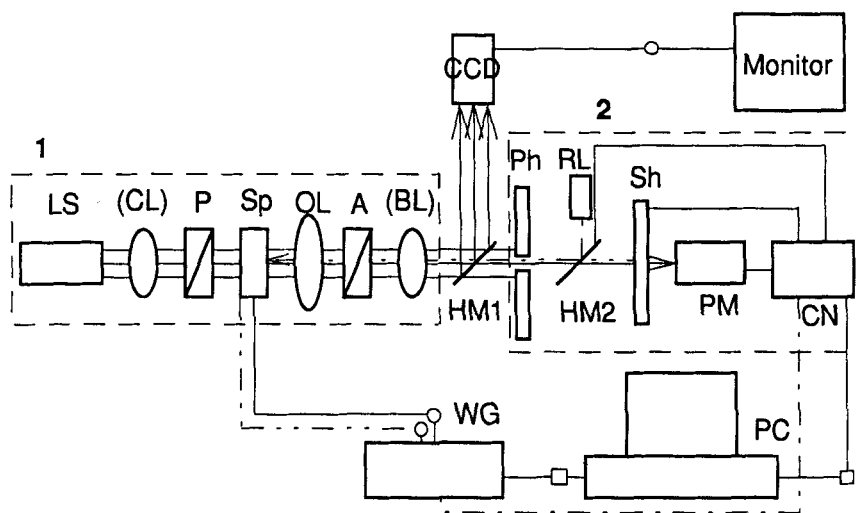


FIGURE 5 The instrument used for domain transition observation.

LS:Light source, CL:Condenser lens, P:Polarizer, SP:Sample, OL:Objective, A:Analyzer, BL:Bertrand lens, Ph:Pin holes, HM:Half mirror, RL:Reference light, Sh:Shutter, PM:Photo-multiplier, CN:Controller, WG:Arbitrary wave generator, PC:Personal computer

To find the LC director alignment, transmittance was measured with the photo-multiplier unit (2) by shifting pin holes (Ph) on the conoscopic figure. These pin holes sizes are from 0.1mm to 3mm and the corresponding spot sizes on the sample surface are from $2\mu\text{m}$ to $750\mu\text{m}$.

Transmittance was measured on the multi-domain TN sample having the C-TN configuration⁴, in which the domains consist of the TN configuration (Domain 1) and the splayed TN (Domain 2), Domain size is $137\mu\text{m}$ high \times $116\mu\text{m}$ wide. Figure 6 shows transmittance measurement examples on the conoscopic figure for this C-TN sample, where the sample surface spot size is $17.5\mu\text{m}$ in diameter. The horizontal axis represents the applied voltage and the vertical axis

represents the normalized transmittance on a logarithm scale. Figure 7 shows the measuring point geometry, where the transmittance is measured at each hatched circle, located at a center and at the 35° zenith points on the conoscopic figure. In the voltage range, from 0V to 7V, all transmittances varied smoothly. The transmittances measured at up and down spots similarly depend on applied voltage, and so do the transmittances measured at right and

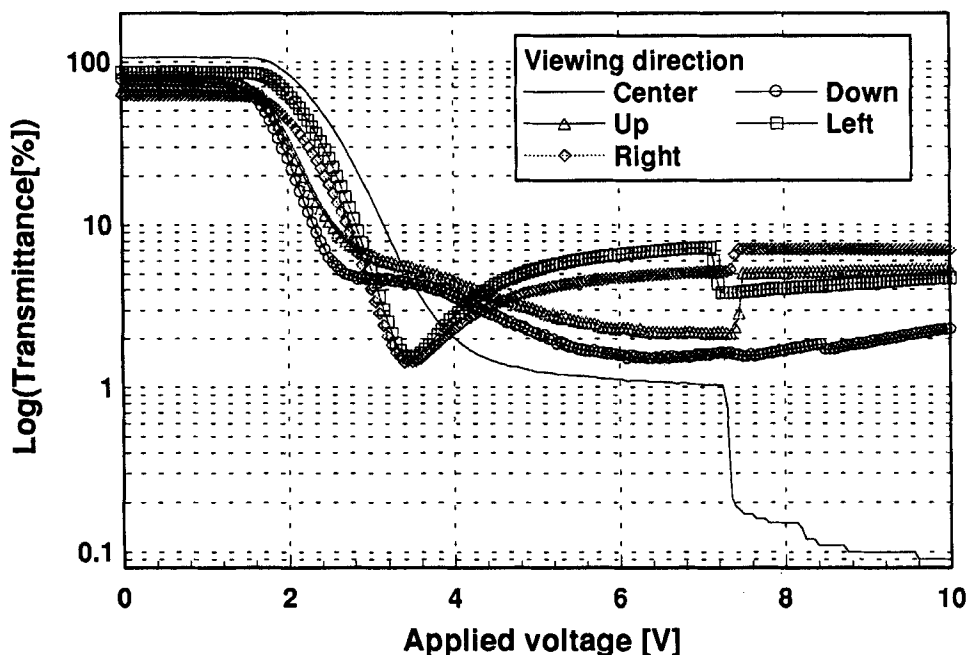


FIGURE 6 Transmittance as a function of applied voltage and measured position on the conoscopic figure.

left spots. The corresponding mid-plane LC director configuration for this result is shown in Figure 8 (a). In this configuration, Domain 1 is the conventional TN structure, shown in Figure 1 (a), and Domain 2 is the splayed TN structure, shown in Figure 1 (b).

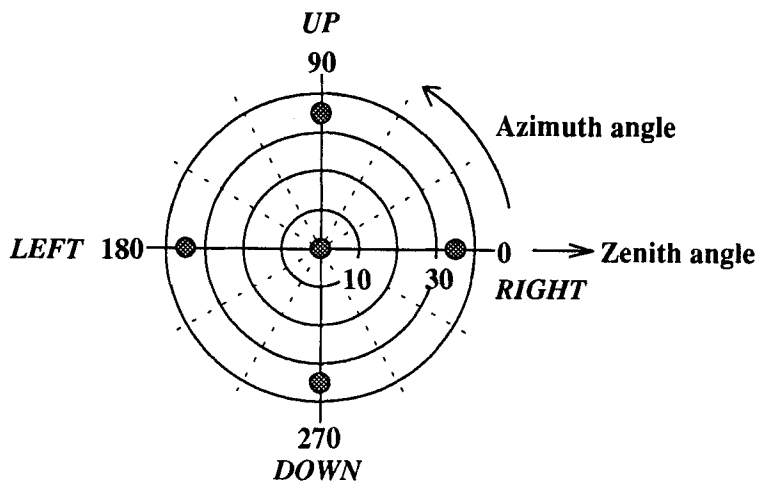


Figure 7 Measured points, represented by hatched circles on the conoscopic figure

The central position transmittance drops suddenly at about $7.4V$, as shown in Figure 6. The domain transition occurs at this voltage, which the authors name as the transition voltage. At this voltage, the transmittances for up and right-hand spots rise sharply. In contrast,

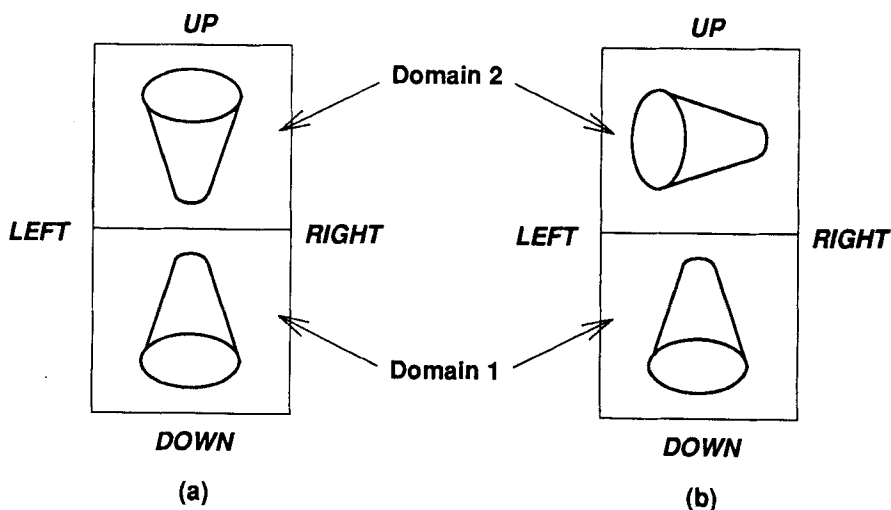


Figure 8 The possible mid-plane LC configurations top views (a) Before transition (b) After transition

the transmittance for left-hand spot drops suddenly. These phenomena are explained quit well by assuming in Domain 2 the transition from the splayed TN configuration to that of the reversely-twisted TN occurs at this transition voltage. Figure 8 shows the corresponding mid-plane LC director configuration (a) before the transition and (b) after the transition. The symmetrical structure (Figure 8 (a)) has changed to the asymmetrical structure (Figure 8 (b)). Based on these results, we conclude that the domain after transition is a reversely-twisted domain.

Definition of the balanced voltage in the experiment

The transition voltage V_r is the experimentally obtained voltage at which the domain transition occurs, but this

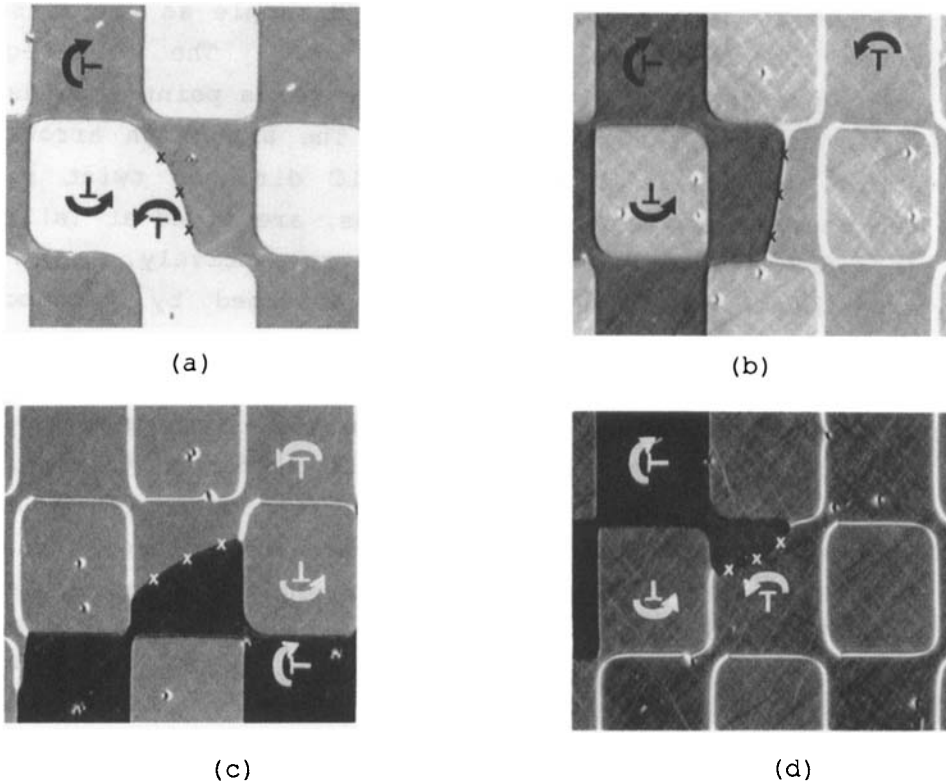


FIGURE 9 Various domain equilibrium states photographs for the C-TN, in the crossed-Nicols observation

voltage differs from the previously mentioned balanced voltage in the simulation. The transition occurs only when the sufficient total energy difference exists to cause a sudden transformation. Therefore, the transition voltage is always higher than the balanced voltage. At the balanced voltage boundary between the splayed TN domain and the reversely-twisted domain doesn't move to either side, because the two energies are exactly the same. Furthermore, in the voltage range lower than the balanced voltage, the transition never occurs spontaneously without some other external field, such as the lateral field⁷ or the pressure.

Figure 9 shows photographs of the various fixed boundaries between the splayed TN domain and the reversely-twisted TN domain for the same C-TN sample as previous one under the crossed-Nicols observation. The LC directors are represented by the nails, whose heads point towards the observer from the paper plane. The arcs with arrowheads around the nails represent the LC director twist sense. The boundaries, marked with crosses, are fixed at (a)3.24V, (b)3.65V, (c)4.12V and (d)4.60V, respectively. In the experiment, the boundaries are affected by neighboring domains and walls. On the other hand, in the simulation the balanced voltage is obtained from one-dimensional system and not affected by neighborhood. The neighborhood effects in the experiment cause the different voltages, at which the boundaries are fixed, correspond to the boundary states shown in Figure 9. However, all voltages obtained from Figure 9 show same dependency on the twist angle and the chiral pitch. We defined the voltage of the state, shown in Figure 9 (b), as the balanced voltage in the experiment for further investigations.

Comparison with the simulation

Figure 10 shows the balanced voltage in the experiment as a function of the chiral pitch and the twist angle for the C-TN sample. The pretilt angles, measured by the crystal

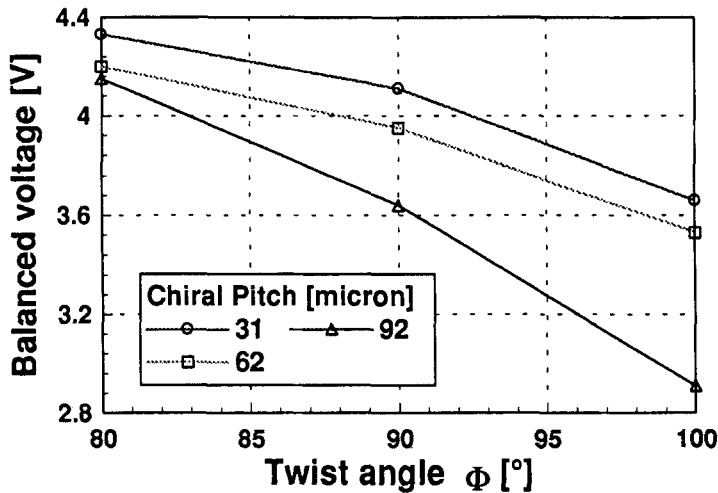


Figure 10 Balanced voltage in the experiment, as a function of twist angle and chiral pitch

rotation method, were about 1.0° for the top substrate and about 6.0° for the bottom substrate. These balanced voltage data are the average values for three cells and the difference between cells is less than $\pm 0.03V$. As the figure indicates, the shorter chiral pitch and the narrower twist angle stabilize the splayed TN configuration. This result qualitatively agrees with the simulation result, shown in Figure 3. The domain stability can be evaluated with this balanced voltage.

APPLICATION

In the device application, contrast ratio should be considered in addition to the domain stability. Based on the energy simulation and transmittance simulation⁸, the condition was found wherein both high contrast ratio and the domain stability are satisfied.

Contrast ratio with stable domains

Figure 11 shows the chiral pitch and the twist angle effect on the contrast ratio plotted against applied voltage for the splayed TN. The pretilt angles are set to the same values as those in the previous simulation. As the figure indicates, the longer chiral pitch and the wider twist angle lowered the voltage for high contrast ratio. This tendency preferable for the contrast ratio is quite opposite to that preferable for the stable domains. In

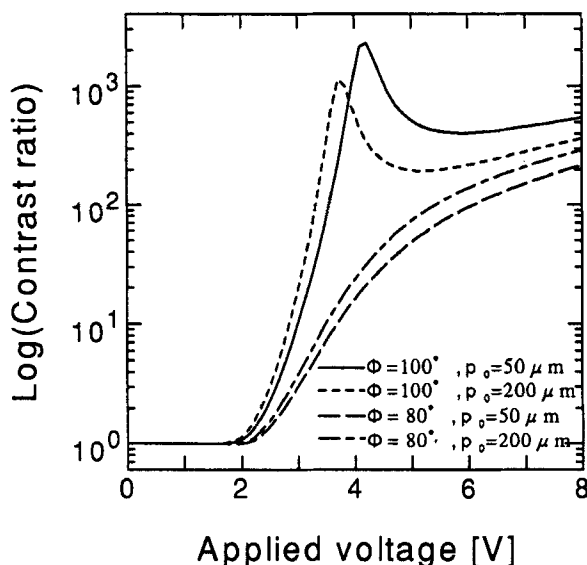


FIGURE 11 Chiral pitch and the twist angle effect on the contrast ratio versus voltage curves for the splayed TN in the simulation.

contrast to this, the effects of the pretilt angle for the contrast ratio and for the stable domains show the same tendency.

The authors further investigate the condition where the highest contrast ratio and stable domains are achieved. Figure 12 shows the contour diagram for the highest contrast ratio with stable domains as a function of chiral pitch and twist angle. From this figure, the contrast ratio over 100 is obtained in the region with shorter

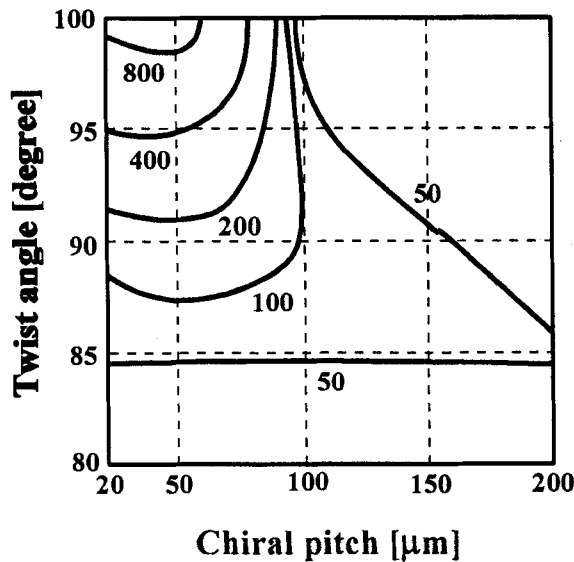


FIGURE 12 Contour diagram for the highest contrast ratio with stable domains as a function of chiral pitch and twist angle in the simulation.

chiral pitch than about $100\mu\text{m}$ and wider twist angle than about 88° . This area varies with the pretilt angle and lower pretilt angles widen this area.

CONCLUSION

The splayed TN configuration stability in the multi-domain TN cell was investigated by both simulations and experiments. The configuration after transition proved to be the reversely-twisted TN configuration, from a transmittance measurement on the conoscopic figure. The splayed TN stability proved to be evaluated by the balanced voltage, which refers to (1) the voltage at which the same LC bulk energy for two possible configurations occurs in the simulation and (2) the voltage at which the boundary between splayed TN and reversely-twisted TN in the experiment is fixed. Narrower twist angle, shorter chiral

pitch and lower pretilt angles raise the balanced voltage, i.e., stabilize splayed TN configuration. Furthermore, the conditions to obtain a high contrast ratio with stable domains are discussed.

REFERENCES

1. M. Yaguchi, Japanese Patent Publication, No.48723 (1983).
2. K. H. Yang, IDRC'91 Digest, pp.68-71 (1991).
3. Y. Koike, T. Kamada, K. Okamoto, M. Ohashi, I. Tomita, M. Okabe, SID'92 Digest, pp.798-801 (1992).
4. K. Takatori, K. Sumiyoshi, Y. Hirai, S. Kaneko, Japan Display'92 Digest, pp.591-594 (1992)
5. A. Lien, R. A. John, SID'93 Digest, pp.269-272 (1993)
6. M. E. Becker, J. Nehring, T. J. Scheffer, J. Appl. Phys., 57, p.4539 (1985)
7. Alan Sussman, J. Electrochem. Soc., 126, No.1, pp.85-89 (1979)
8. A. Lien, SID '91 Digest, pp.586-589 (1991)